FLOODPLAIN LAND COVER CLASSIFICATION

AND CHANGE DETECTION ANALYSIS FOR

THE CITY OF AUSTIN, TX FROM 2008 TO 2016

by

Mackenzie Carhart, B.S.

A directed research report submitted to the Geography Department of

Texas State University in partial fulfillment

of the requirements for the degree of

Master of Applied Geography

with a specialization in Geographic Information Science

May 2018

Committee Members:

Dr. Ronald Hagelman III, Committee Chair

Dr. Jennifer Jensen, Committee Member

FLOODPLAIN LAND COVER CLASSIFICATION

AND CHANGE DETECTION ANALYSIS FOR

THE CITY OF AUSTIN, TX FROM 2008 TO 2016

by

Mackenzie Carhart, B.S

May 10, 2018

TABLE OF CONTENTS

ACKNOWLEDGMENTS

As my research advisor, Dr. Ronald Hagelman III, continuously reminded me throughout the course of my graduate career, a task or project of any caliber requires assistance and feedback from a dependable and well-informed team. I would like to express my sincerest appreciation and gratitude toward several individuals who supported my thoughts and ideas, research, and educational pursuits over the last several years.

First, I would like to thank my research advisor for his unfailing guidance, wisdom, and humor that encouraged me to pursue a Master's degree and complete graduate coursework and research of which I am extremely proud.

Second, I would like to thank my committee member, Dr. Jennifer Jensen, for her valuable advice and contributions during the image classification and analysis process of my research. This study would not be as thorough or illustrative without her assistance.

Third, I would like to thank my friend and peer from the Department of Geography, David Szpakowski, for his willingness to help troubleshoot various issues and concerns throughout the course of my research.

Lastly, I would like to express my deepest love and gratitude to my family and friends who were the mental and emotional backbone of my entire graduate career. Their empathy, kindness, and unwavering motivation fueled my educational pursuits, and I could not be more appreciative for them.

LIST OF TABLES

LIST OF FIGURES

LIST OF ABBREVIATIONS

AOI	Area of Interest
CIR	Color-Infrared
EPA	Environmental Protection Agency
FEMA	Federal Emergency Management Agency
NAIP	National Agricultural Imagery Program
NC	Natural Color
TX	Texas
TxDOT	Texas Department of Transportation
TNRIS	Texas Natural Resource Information System
USDA	United States Department of Agriculture
USGS	United States Geological Survey

I. PROBLEM IDENTIFICATION AND EXPLANATION

In the rapidly expanding region of central Texas, the unique grouping of flash flood-prone physiography and vulnerability to extreme meteorological circumstances has catalyzed major flood events throughout the last century (Furl et al. 2015). As heavily urbanized areas such as the City of Austin, TX continue to expand their reach and influence across the region, increases in impervious surfaces can exacerbate the potential for extreme flooding (Furl et al. 2015). If these infrastructural changes fall within the city's 100 and 500-year floodplains, they can affect the overall magnitude of an extreme hydrometeorological event.

Established and enforced by the United States Federal Emergency Management Agency (FEMA) in the 1960s, a 100-year floodplain is a statistical probability tool that outlines the area of land that is predicted to flood during a "100-year storm" (City of Austin 2016). This storm has a 1% chance of occurring in any given year and, if and when such storms occur, they can generate catastrophic damage if landscape and meteorological circumstances are just right. Similarly, a 500-year floodplain is a statistical probability tool that defines segments of land that are subject to flood during a "500-year storm" (FEMA 2017). This storm has a 0.2% chance of occurring in any given year. In order to understand the potential hazards[1] that are commonly associated with major flood events in urbanized floodplains, research must consider the distribution and relationships between the various land cover characteristics present.

[1] A hazard is something that has the potential to cause harm but does not necessarily do so (Flood Risk Management 2017).

II. SITE AND SITUATION

The geographic setting for my research study is the City of Austin, TX. Nestled between the Balcones Escarpment and the bustling I-35 corridor of Central Texas, Austin boasts a land coverage of over 271 square miles of rolling hills, congested roadways, and sprawling urban growth (City-Data.com 2017). In addition, Austin reigns as the capital city of the Lone Star State and the "Live Music Capital of the World" (City of Austin 2017c). In total, the breadth of the city encompasses territory that spans across portions of two different counties, including Travis and Williamson Counties.

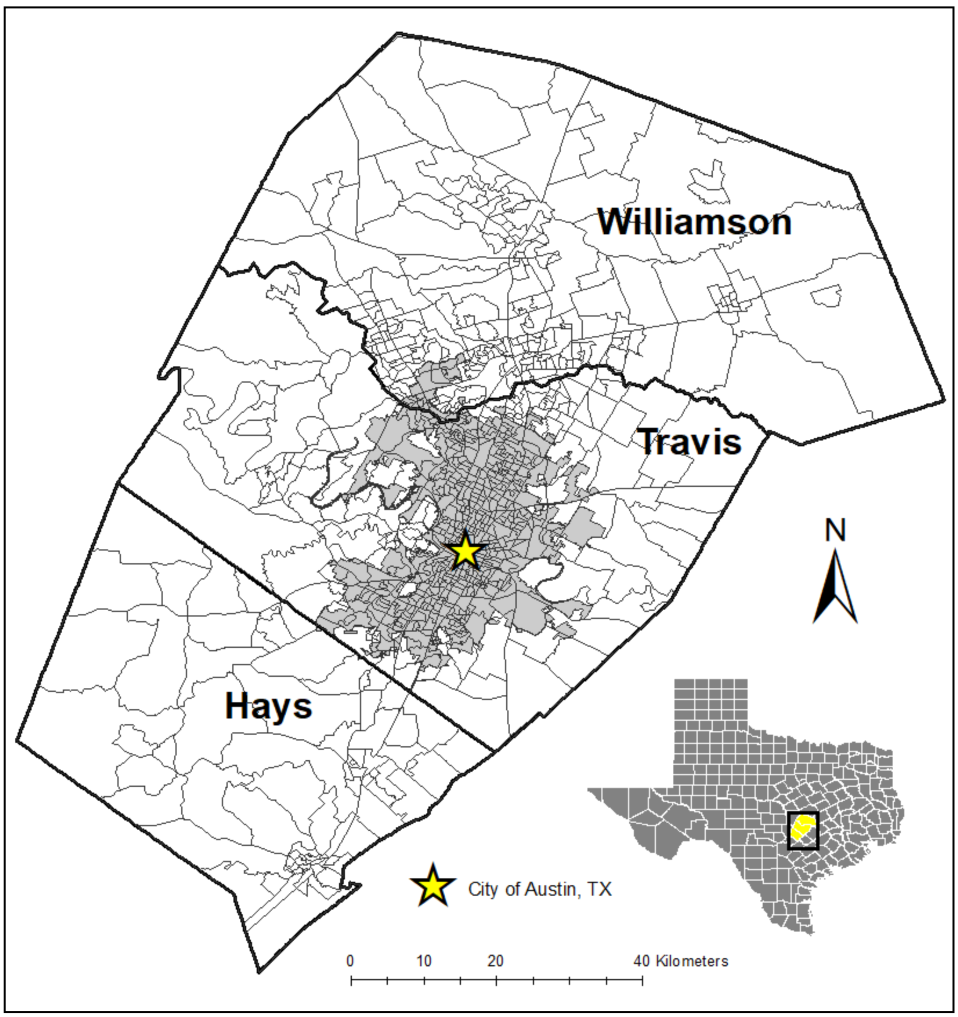

Figure 1. Area of Interest. The city limits and block groups of Austin, TX.

The City of Austin also sits at the heart of the Austin-Round Rock-San Marcos Metropolitan Statistical Area (MSA), which was estimated to have a population of more than 2 million people in 2016 (U.S. Census Bureau 2017). Given its rapid growth, diverse physical landscapes, and eclectic culture, Austin lies at the forefront of a movement to become the next great American metropolis.

From scenic views to countless recreational activities, Austin grants natives, newcomers, and tourists alike the opportunity to immerse themselves in the beauty and culture that Central Texas has to offer. The city sits along on the Lower Colorado River and has five large artificial lakes located within the city limits. These lakes include Lady Bird Lake, Lake Austin, Lake Travis, Lake Walter E. Long, and the Soil Conservation Service Site 7 Reservoir (Table 1). In addition, numerous rivers and streams surround the Greater Austin Area (Table 2). While the east side of the city is relatively low-lying, the west side of the city features rolling hills and limestone-rich, clay loam soil (Texas State Historical Association 2017). The climate and vegetation characteristics native to this region are largely a product of the geographic positioning of the city in relation to the rest of the state and country. For the most part, Austin has a humid subtropical climate (Texas State Historical Association 2017). The city, however, sits along a climatic transition zone, so it can occasionally experience a mixture of both semi-arid and humid subtropical climates. Under specific hydrometerological conditions, this characteristic can often produce torrential rainfall and flash flooding throughout the region. As the effects of climate change continue to surface and intensify across the landscape, attention will need to be drawn to the potential environmental hazards that could negatively influence the city, such as droughts and flash flood events (Green et al. 2000).

Water Body Name	Area (km²)	Elevation (m)
Lady Bird Lake	1.96	130.5
Lake Austin	5.72	25.28
Lake Travis	72.85	207.59
Soil Conservation Service Site 7 Reservoir	.194	246.29
Walter E. Long Lake	4.93	169.2

Table 1. Water Bodies in the Study Area. Name, area, and elevation of five major water bodies located within the 100 and 500-year FEMA floodplains in Austin, TX.

River or Stream Name	Length (km)	River or Stream Name	Length (km)
Barton Creek	13.16	Hucks Slough	.734
Bear Creek	5.46	Johnson Branch	3.07
Bee Creek	.126	Laurel Oaks Creek	6.15
Blunn Creek	4.68	Little Bee Creek	.874
Boggy Creek	21.32	Little Walnut Creek	13.71
Bull Creek	12.49	Marble Creek	5.66
Carson Creek	8.29	Mayfield Creek	.486
Coldwater Creek	.423	Onion Creek	37.84
Colorado River	67.53	Rinard Creek	3.69
Connors Creek	2.48	Shoal Creek	16.37
Cottonmouth Creek	.937	Skunk Hollow Creek	1.12
Country Club Creek	6.29	Slaughter Creek	18.44
Cow Fork	2.89	Tannehill Branch	7.99
Decker Creek	5.25	Tar Branch	1.8
Dry Creek	5.25	Turkey Creek	4.12
East Bouldin Creek	3.48	Waller Creek	10.83
Elm Creek	2.01	Walnut Creek	34.57
Ferguson Branch	3.19	Wells Branch	2.7
Furtado Creek	2.43	West Bouldin Creek	2.78
Hancock Creek	3.32	West Bull Creek	4.83
Harris Branch	10.54	Williamson Creek	17.51
Hog Pen Creek	.929	Null Values (693)	516.62
Honey Creek	.687	**Total Length**	894.63

Table 2. Rivers and Streams in the Study Area. Name and length of 736 river and stream systems located within the 100 and 500-year FEMA floodplains in Austin, TX.

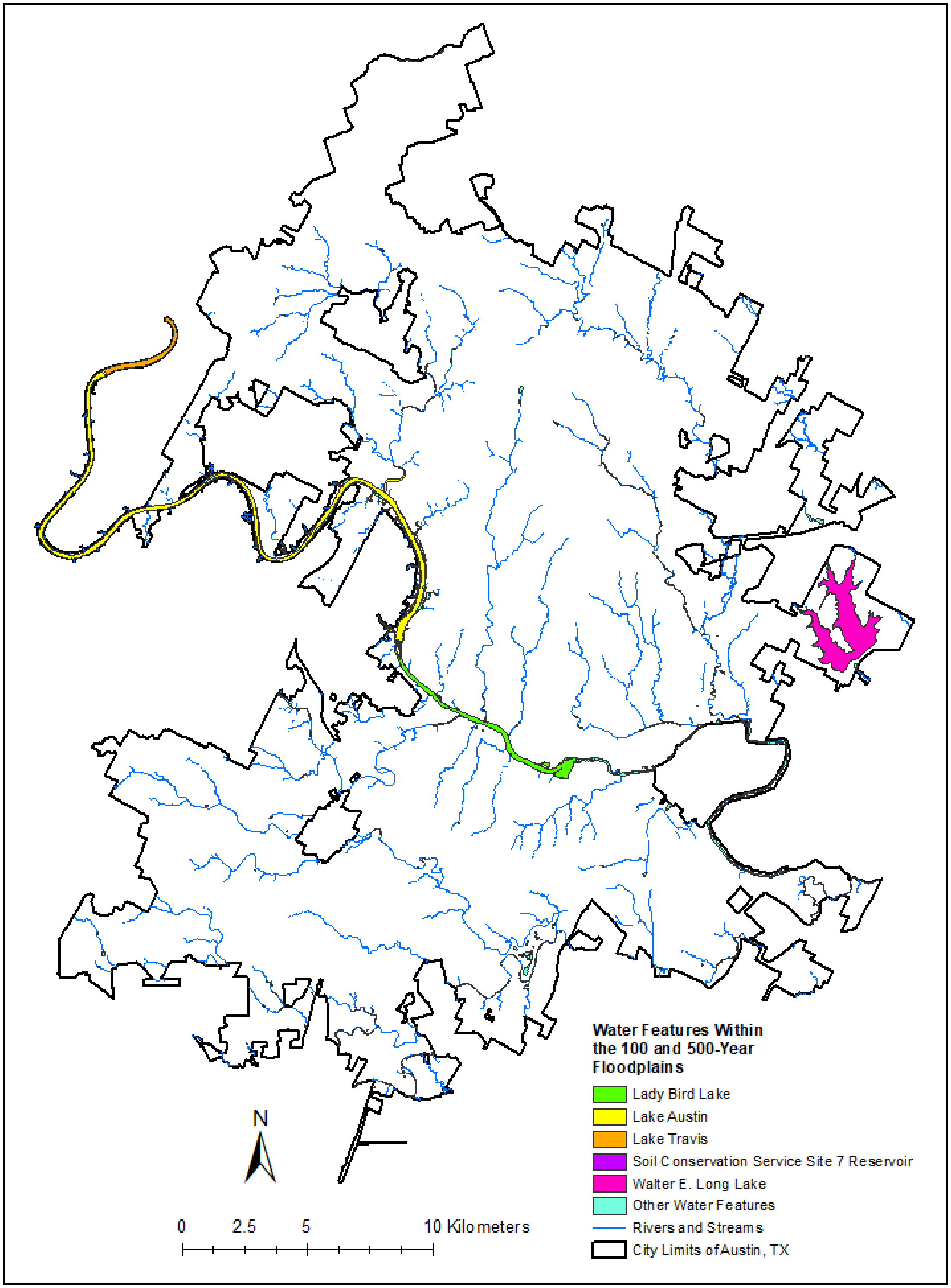

Figure 2. Major Hydrological Features. Water bodies, rivers, and streams located within the study area of the 100 and 500-year FEMA floodplains in Austin, TX.

As the 4th-most populous city in the State of Texas and the 11th-most populous city in the United States, the City of Austin is amongst the fastest-growing cities in the nation (U.S. Census Bureau 2017). According to the United States Census Bureau, Austin experienced a 12% increase in population from 2010 to 2013 (U.S. Census Bureau 2017). In January of 2017, *Forbes Magazine* labeled Austin as the fastest growing city in the U.S., and the *U.S. News and World Report* named Austin the best place to live in the nation (Forbes 2016a and U.S. News and World Report 2017).

With a thriving technology sector, an active, forward-thinking population base, and a relatively low cost of living, Austin possesses a unique gravitational pull that most American cities wish to have. Because of this, the city has been experiencing a consistent annual increase in population growth within recent years. According to the U.S. Census Bureau and the City of Austin, the city boasted a population of approximately 926,426 individuals in 2016, which was a 2.9% increase from the previous year (U.S. Census Bureau 2017). Austin has a population density of 3,358 people per square mile, and a median age of 31.8 years (U.S. Census Bureau 2017). The population is comprised of 49.60% female and 50.40% male (U.S. Census Bureau 2017). In addition, the income per capita is $32,672, and the median household income is $55,216 (U.S. Census Bureau 2017). With a young, educated, and ambitious demographic base, the City of Austin will continue to stand out amongst the rest as it paves the way to ensure that it will become a promising city of the future.

III. LITERATURE REVIEW

Due to the recent increase of interest in land development within urbanized floodplains, the breadth of existing literature on the topic is extremely narrow. However, the literature relevant to this study was informative, comprehensive, and supported by both quantitative and qualitative research methods. Of the existing literature reviewed, many acknowledged that floods are one of the most common types of environmental disasters throughout the world (Green et al. 2000, Kiedrzyńska et al. 2015, and Kwak et al. 2008). Not only are they caused by natural phenomena (i.e. hydrometerological events or climatic trends), but they can also be a result of anthropogenic factors (i.e. rapid and unfettered urbanization, land erosion, lack of flood mitigation efforts, etc.) (Glosińska 2014 and Green et al. 2000). One of the most common forms of anthropogenic intrusion is urban growth, especially near or within floodplains (Kourgialas et al. 2011). Of Because of this, floods can quickly intensify and, as a result, produce large-scale losses across multiple realms, including local and regional infrastructure, environmental degradation, public and private property damage, and human lives (Kiedrzyńska et al. 2015).

Risk is defined as the probability of an event happening and the impact if it were to occur (Li et al. 2016). The risk of flooding is a major concern amongst governing entities throughout the world, and recent evidence has shown that human activities and interference within the floodplain can actually instigate an increased frequency of extreme flood events (Green et al. 2000, Kiedrzyńska et al. 2015, and Kwak et al. 2008). This problem is even more severe in developing cities where there is poor regulation over land use practices and ordinances within floodplains (Antonie et al. 1997 and Ndabula et al. 2012). In recent decades, the research surrounding floodplain analysis and management has largely focused on the effects of flooding in these federally defined areas, especially as they relate to the environment and human life.

Of the literature that is relevant to this study, much of it relates to describing the urbanized floodplain as being an attractive area of settlement that underwent rapid and chaotic development (Green et al. 2000 and Li et al. 2016). As a result of this ongoing expansion, catastrophic floods that produce serious material and human losses are becoming more and more common (Green et al. 2000 and Kiedrzyńska et al. 2015). This shift in flood risk throughout urban zones is a direct effect of the improper management of flood-prone areas by city officials, developers, and residents (Glosińska 2014). In order to predict and mitigate the possible impacts of major flood events, steps must be taken to identify the primary forms of land usage within the floodplain as well as the contiguous characteristics that define the specific area (Glosińska 2014).

Furthermore, many studies regarding the effects of floods on urbanized floodplains suggest that much of the accumulated damage is socio-economic in nature (Aubrecht et al. 2010). This includes, but is not limited to, damage to infrastructure, temporary suspension of public and private services (i.e. sewage treatment, factory operations, garbage pick-up, etc.), loss of structural property (i.e. residential homes and businesses), temporary or permanent displacement of residents, and reliance on borrowed capital for efforts centered on clean-up and rebuilding (Green et al. 2000). The potential for loss is great in urbanized floodplains during a flood event, and many could experience an increase in hazards depending on future land development or rehabilitation in the area.

A not-so-surprising pattern that surfaced amongst the literature reviewed was the researchers' keen acknowledgement of the looming threat of climate change on future flood events (Kwak et al. 2008). As urban areas continue to experience intensifying climatic patterns and population growth, city officials, developers, and residents will need to adjust their perceived risks to flood hazards accordingly (Glosińska 2014). In fact, the impacts of climate change may eventually require an outward expansion of the 100 and 500-year floodplains to ensure that areas statistically predicted to flood receive the education, outreach, and protection concerning the potential hazards that they may face (Nel et al. 2014). Moreover, the imminent threat of climate change serves as a rather convincing catalyst for conducting a land cover classification and change detection analysis and, in response, addressing the landscape characteristics within flood-prone areas that could be most affected by a major flood event.

As noted, while the processes of extreme hydrometeorological events in central Texas have been thoroughly explored and documented within recent years, a comprehensive land cover classification and change detection analysis of the City of Austin's 100 and 500-year FEMA floodplains has not yet been done. Of the literature reviewed, many of the articles suggest that the rapid urban development that is taking place within floodplains is largely a result of poor land use planning and management. Still, no research has cataloged the specific land cover types across the floodplain, as well as how they may affect the possible risks and hazards associated with flood events. As such, this study fills a significant gap in the existing research.

IV. RESEARCH OBJECTIVES

The general objective for this study is to create a land cover classification and change detection analysis of the federally declared 100 and 500-year FEMA floodplains in the City of Austin, TX from 2008 to 2016. This will be achieved through the following specific objectives:

- Create two digitalized floodplain maps of the study area in 2008 and 2016 using high resolution, compressed county mosaic images and a geospatial software program, such as Esri ArcGIS;
- Classify the land cover types of the two images using a supervised approach in a remote sensing software program, like ERDAS Imagine;
- Calculate and compare the percent change of land cover classifications between 2008 and 2016 within the study area using analysis techniques that are supported by a remote sensing software program, like ERDAS Imagine;
- Produce multiple maps that illustrate the distribution and change of land cover types within the study area during the given timeframe.

This study seeks to answer the following questions: What are the land cover characteristics of Austin's 100 and 500-year FEMA floodplains and how has the landscape of the urbanized floodplain changed throughout the given timeframe? Each portion of the research objective seeks to facilitate an increased understanding of the types of surface cover that exist within the floodplain. As a result of this study, I argue that there will be a lack of variety amongst the land cover types throughout the city's urbanized floodplain. In addition, I argue that the floodplain will have had undergone an increase in land cover change and development between the years of 2008 and 2016.

Although research has been previously conducted on the effects of various hydrometeorological events in this particular region of Texas, a land cover classification and change detection analysis of the City of Austin's 100 and 500-year FEMA floodplains have not yet been done. With growing concerns surrounding the impending threats of climate change on heavily populated and expanding urban environments, I believe that city officials, developers, residents could greatly benefit from the results of this study. Equipped with an increased awareness of what actually exists in the floodplain, I hope that they will then be prepared to make responsible decisions concerning future efforts in land development and flood hazard mitigation and management.

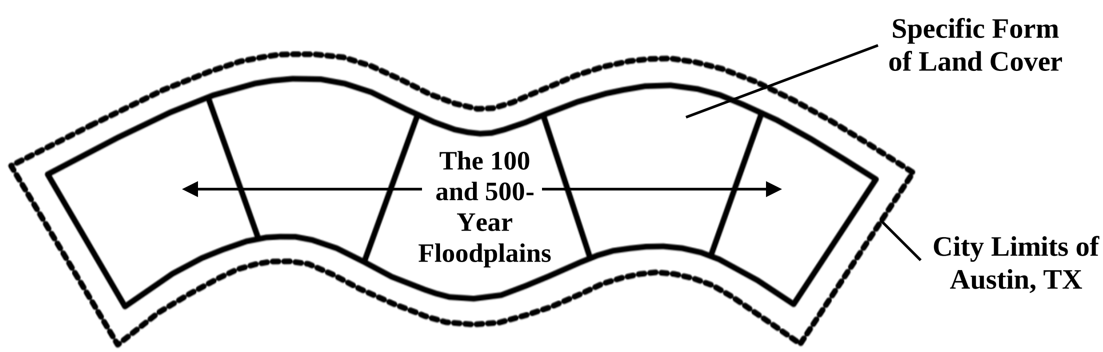

Figure 3. Conceptual Model for the Study Area. The FEMA 100 and 500-year floodplain boundaries within Austin, TX and forms of land cover found within the study area. Created by Dr. Ronald Hagelman III and Mackenzie Carhart, 2016.

V. METHODOLOGY AND PROCEDURES

As stated in the research objectives, the purpose of this study is to create a land cover classification and change detection analysis of the 100 and 500-year FEMA floodplain in the City of Austin, TX. A positivist epistemology was incorporated to unearth the locations and characteristics of specific types of land cover across the region. These forms of land cover illustrates the linkages hypothesized to be critical in understanding how the human activities, or lack thereof, distributed throughout the floodplain boundaries can alter– either positively, negatively, or none at all – the identity of the urbanized landscape (Figure 3). The variables establish the general topographic characteristics and identity of areas within the urbanized floodplain of the City of Austin (Table 3).

Observed Variables	Source of Data	Type of Data	Year Published
Orthographic Imagery	NAIP and TNRIS	Raster	2008 and 2016
City Limits of Austin, TX	TxDOT	Vector - Polygon	2016
Water Bodies	USGS, EPA, and TNRIS	Vector - Polygon	2009
Rivers and Streams	USGS, EPA, and TNRIS	Vector - Line	2009
Floodplain Boundaries	FEMA	Vector - Polygon	2017

Table 3. List of Observed Variables. Five forms of data used for this research study, as well as the sources, types, and year the data was published.

To conduct an accurate and thorough land cover classification and change detection analysis of the 100 and 500-year floodplain in the City of Austin, the research question and objectives were approached in three major steps: data collection and preparation, digital extraction and mapping of the FEMA 100 and 500-year floodplains from orthographic imagery and geospatial datasets, and a land cover classification and change detection analysis of the urbanized floodplain by using remote sensing software.

5.1 Data

First, the necessary data was acquired from their appropriate state and federal agencies. Given the nature and study area of this project, much of the data was supplied through TNRIS, TxDOT, USGS, EPA, and FEMA (Table 3). Each orthographic image was produced by NAIP as a high resolution, compressed county mosaic of Travis County and provided for free and immediate download by TNRIS, a division of the Texas Water Development Board. Administered by the USDA Farm Service Agency's Aerial Photography Field Office, NAIP obtains aerial imagery during the agricultural growing seasons throughout the U.S. The two images were photographed in 2008 and 2016 at a 1-meter pixel resolution with either three or four bands (United States Department of Agriculture). The image from 2008 is CIR with four bands, including red, green, blue, and near infrared. The image from 2016 is NC with three bands, including red, green, and blue. As per NAIP's image acquisition specifications, each image was photographed with no more than 10% cloud cover per quarter quad tile (United States Department of Agriculture).

Lastly, TxDOT provided the city limits of Austin, TX, and FEMA supplied the floodplain boundaries as a flood zone shapefile (Table 3). As per the FEMA flood zone guidelines, zones A, AE, and AO are categorized as the 100-year floodplain and zone X as the 500-year floodplain (Figure 4). TNRIS, USGS, and EPA provided the location and boundaries of the water bodies, rivers, and streams in the form of a single geodatabase.

As noted in Table 3, the water bodies are polygon features and the rivers and streams are line features.

In the second step of the project, Esri's ArcGIS was utilized to define the study area in each of the orthographic images. First, the cells of each raster file were outlined to the city limits of Austin by using the "Extract by Mask" tool. Then, the 100 and 500-year floodplain boundaries within the FEMA flood zones layer were consolidated into a separate layer. Afterwards, the new floodplain layer was clipped to the city limits of Austin to define the extent of the study area. Then, the boundaries of the 100 and 500-year FEMA floodplains in each raster file were clipped to the city limits of Austin by utilizing the "Extract by Mask" tool. Finally, the major waterbodies, rivers, and streams were erased from each image using the "Extract by Mask" tool and a polygon feature that included the water systems throughout the study area (Figures 6 and 7). In order to accommodate wider portions of rivers and streams throughout the study area, a 1-meter buffer was applied to the feature. In addition, smaller water bodies (i.e. artificial lakes, retention ponds, municipal fountains, etc.) were extracted from the images using the same methodology. These steps were taken to avoid possible spectral misclassifications between water and developed land in the 2008 image and water and vegetation in the 2016 image. Upon completing these steps, both files were exported as IMAGINE images (.img) and imported separately into ERDAS Imagine for image classification.

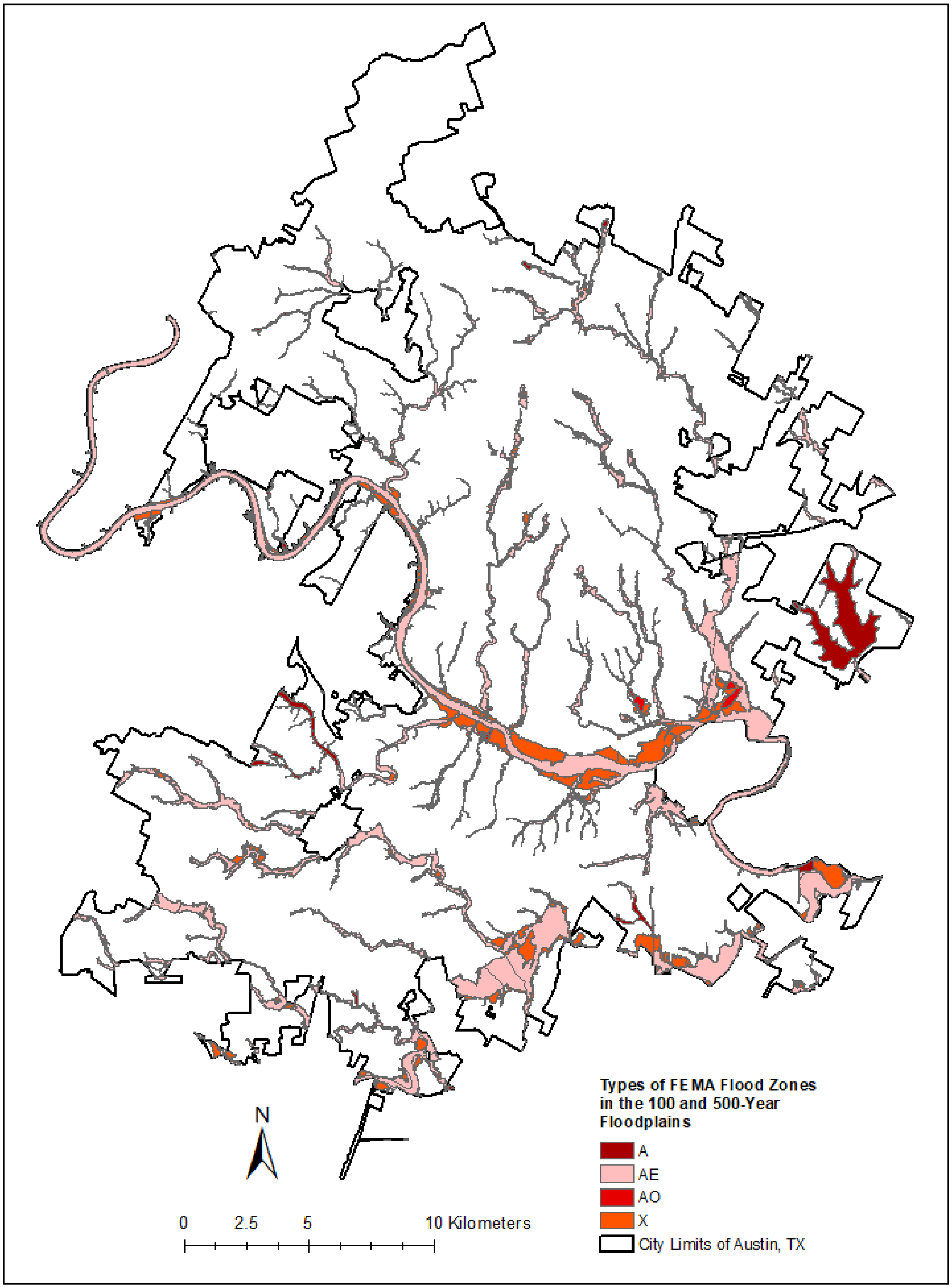

Figure 4. FEMA Flood Zones. Specific types of federally declared flood zones that comprise the 100 and 500-year floodplains in Austin, TX.

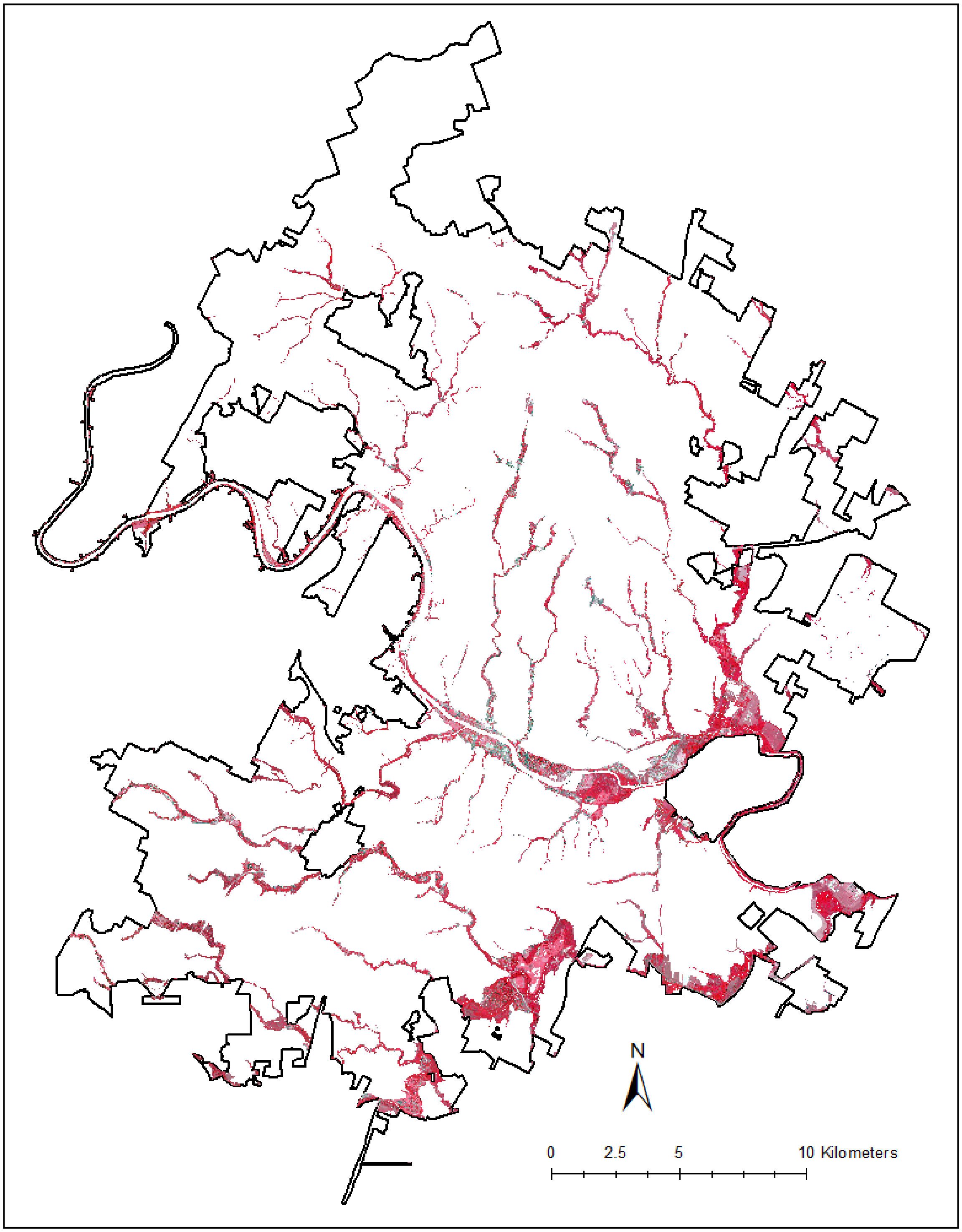

Figure 5. CIR Imagery of the Study Area in 2008. Data used to define the study area, including multispectral imagery, the FEMA 100 and 500-year floodplain boundaries, and the city limits of Austin, TX.

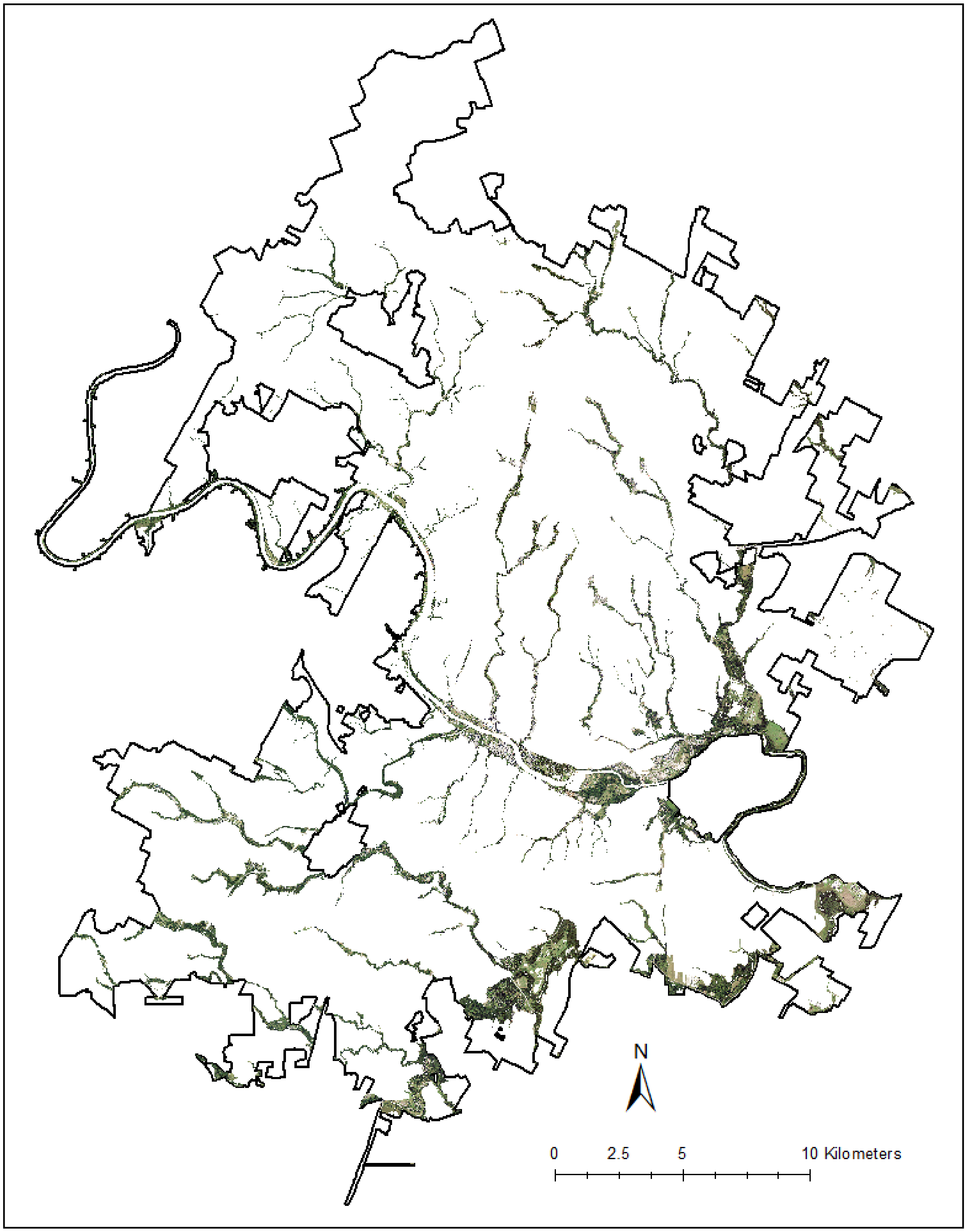

Figure 6. NC Imagery of the Study Area in 2016. Data used to define the study area, including multispectral imagery, the FEMA 100 and 500-year floodplain boundaries, and the city limits of Austin, TX.

Type of Land Cover	Classification Code	Color for Thematic Layer
Vegetation	1	Dark Green
Developed Land	2	Red

Table 4. Land Cover Types and Image Classification Criteria. Two forms of land cover used in this study, as well as their classification codes and thematic colors for image classification analysis.

Next, the primary forms of land cover that are relevant to the objectives of this study were identified (Table 4). To do this, the Anderson Land Classification Scheme was referenced. Established in 1976 by USGS, the system is a standardized classification scheme that is used by local, state, regional, and federal entities in the identification of land use and land cover types throughout the United States with remote sensing techniques (Anderson 1976). For the purposes of this study, vegetation and developed land were the only forms of land cover included in the image classification and analysis.

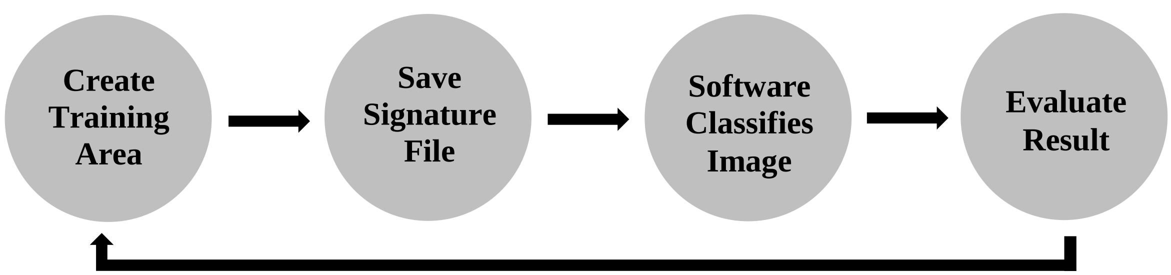

Figure 7. Conceptual Model Supervised Classification Process. The flow of events required to execute a supervised classification in ERDAS Imagine.

In remote sensing, classification is the process by which the pixels of a multispectral image are grouped together based on their data values (Sisodia et al. 2014). In order to assert greater user control over the characterization of the pixels in each image, this study utilized a supervised maximum likelihood classification. A supervised classification requires the user to "supervise" the classification process by specifying the specific pixel values and spectral signatures (i.e. AOI) that are associated with each class (Humboldt State University). Upon creating a representative sample for each class, the software then uses the "training areas" to classify the entire image based on the parametric rules chosen by the user (Figure 7). This study incorporated a maximum likelihood classification algorithm, which assumes that the values assigned to each class are normally distributed, and assigns each pixel to the class that exhibits the highest statistical probability (Sisodia et al. 2014).

Year of Image Acquisition	Image Type	Type of Land Cover	Number of AOIs
2008	CIR	Vegetation	445
		Developed Land	300
2016	NC	Vegetation	475
		Developed Land	350

Table 5. AOIs Gathered by Image and Land Cover Class. Amount of AOIs gathered for each land cover type in the 2008 and 2016 images.

By utilizing the polygon-drawing tool in ERDAS Imagine, several AOIs were created for two specific land cover types that exist across the study area (Table 5). Then, the individual AOIs for each type of land cover were merged into one AOI, assigned each form of land cover a specific color, and saved the set as a separate signature file for each image (Table 4). Upon creating the training sites and signature files, the images were ready to undergo a supervised maximum likelihood classification.

After conducting the classifications, the distribution of classes throughout each output image were observed in ERDAS Imagine. Unfortunately, the pixel values for both the extracted hydrological features and background of the raster output were classified as developed land. To address this issue, the "Erase" and "Extract by Mask" tools in

ArcMap were utilized to remove the water bodies, rivers, and streams from each classified image. Then, the background color was removed by clipping the output layers to the boundaries of the study area (Figures 12 and 13).

Classified 2008 Image		Classified 2016 Image	
Developed Class	Vegetation Class	Developed Class	Vegetation Class
1	445	1	415
Raster Calculator Equations • "Classified_08" == 1 • "Classified_08" == 445		**Raster Calculator Equations** • "Classified_16" == 1 • "Classified_16" == 415	
Raster Calculator Output Files • "Dev08_RasterCalc" • "Veg08_RasterCalc"		**Raster Calculator Output Files** • "Dev16_RasterCalc" • "Veg16_RasterCalc"	

Table 6. Pixel Values and Equations by Image and Land Cover Class. Values of the developed and vegetation classes in each image, as well as equations and output files used to define the pixel values.

To ensure that the images would import into ERDAS Imagine as thematic raster files, the "Raster Calculator" tool was used to specify the pixel value of the land cover classes in each image. The values were from the attribute table of each classified image and assigned to their appropriate class by using the equations shown in Table 6. Upon defining the value for each class, a location was determined for the output file and the equation was performed by the "Raster Calculator" tool.

Pixel Values of Developed Class		Pixel Values for Vegetation Class	
Old Values	New Values	Old Values	New Values
0	1	0	0
1	2	1	2
NoData	NoData	NoData	NoData

Table 7. Reclassified Pixel Values by Land Cover Class. Comparison of old and new values for the developed and vegetation classes in each image.

Then, the “Reclass” tool was utilized to reclassify the pixel values for the vegetation class in each image (Table 7). The values for the developed class did not change. The final values are displayed in Table 8. Once the tool reclassified the pixel values, the “Raster Calculator” tool was used to add the output file of the reclassified vegetation pixels to the output file of the defined developed pixels from Table 6. Once the equation had processed each image, the pixel values and placement of the two land cover classes were observed in both the output image and coordinating attribute table. This was a critical step in the pixel reclassification process because it confirmed the accuracy of the raster calculations. After each image was reviewed, the two files were exported as unsigned, 8-bit IMAGINE images (.img) for further data manipulation in a remote sensing software program.

Classified 2008 Image			Classified 2016 Image		
Developed	Vegetation	NoData	Developed	Vegetation	NoData
1	2	NoData	1	2	NoData

Table 8. Assigned Pixel Values by Image and Land Cover Class.
Final values for the developed and vegetation classes in each image.

Next, the images were imported into ERDAS Imagine. The “Subset” tool was utilized to convert each file into a thematic image. This step was important because it displayed the pixel values and histograms of the two previously defined land cover classes and confirmed that each class was present and accurately distributed throughout the images. Once the tool had processed each file, the pixels values and placement of the land cover classes were observed in the new thematic images. Using the original reference images in Figures 5 and 6 for clarity, the “Inquire” tool was utilized to manually verify the values of random pixels throughout each of the classes. Once the position and distribution of the values were reviewed for general accuracy, the study progressed to the final steps.

5.2 Analysis

Lastly, an accuracy assessment of the two classified images was conducted, as well as a change detection analysis of the two different forms of land cover within the city's 100 and 500-year FEMA floodplains between 2008 and 2016. Given the intricate nature of remotely sensed data, it is imperative to consider and review the dependability of the results upon conducting a classification of one or more thematic images (Congalton 1991). Not only does an accuracy assessment evaluate the quality of a classified image, but it also identifies potential places of error and misinterpretation amongst the pixel values and classes (Foody 2002). A change detection analysis identifies the temporal differences in the condition of an entity or occurrence over a specific period of time (Singh 1989). This technique is useful in a variety of applications, including recognizing changes in land use, seasonal shifts in agricultural production, disaster impacts following a natural or technological hazard, and other environmental alterations (Singh 1989). Because this study involves thematic data, a Matrix Union was used to distinguish differences in developed and vegetation land cover between two images acquired in 2008 and 2016.

The components of the accuracy assessment (i.e. sample size, desired accuracy, and allowable error) were calculated based on a binomial distribution. The equation shown in Figure 8 was used to determine the amount of reference points required for an expected accuracy of 85% and an allowable error of 10% in each image. This study used a stratified random sampling technique to generate 51 points throughout the study area in each image. With a stratified random sample, points are generated according to the division of classes, or “strata”, and their shared attributes or characteristics within the dataset (Gonçalves et al. 2007). In addition, a minimum number of reference points are specified for each class in the image. This study required at least 20 points to be randomly located in each land cover type. Lastly, a maximum of 1,094 pixels were analyzed to determine whether they met the defined conditions of this study.

$$N = \frac{2^2(\mathrm{p})(\mathrm{q})}{\mathrm{E}^2} \qquad\qquad 51 = \frac{2^2(85)(15)}{10^2}$$

Figure 8. Equations for a Binomial Distribution. Used to determine the sample size needed for the accuracy assessments. The equations are largely based on the expected accuracy and allowable error in each image.

As shown in Table 9, the overall classification accuracy of each image is over 90%. In the classified image from 2008, both the producer and user’s accuracies for each class range from 95-100%. The overall Kappa statistic is 0.9585, which suggests that the classification is a 96% better agreement than by chance alone. In the classified image from 2016, both the producer and user’s accuracies for each class range from 80-100%. The overall Kappa statistic is 0.8294, which proposes that the classification is an 83% better agreement than by chance alone. The variation of accuracies and Kappa statistics between the two classified images is likely due to differences in the multispectral characteristics of each reference image used to develop the classification signatures during the supervised classification process.

Along with the accuracy and Kappa statistics, error matrices are provided for each classified image in Table 9. The matrices show the class types determined from the reference and classified images, as well as the sites classified both correctly and incorrectly, according to reference data utilized during the supervised classification and accuracy assessment processes. By referring to the error matrices and a simple equation, one can determine the overall accuracy of the classification, as well as the producer and user's accuracies for each of the class types in either image (Figures 9-11).

$$Accuracy_{Total} = \frac{\text{Number of Correct Plots}}{\text{Total Number of Plots}} \times 100 \qquad 98.04\% = \frac{19 + 31}{51} \times 100$$

Figure 9. Equations for Total Accuracy Calculation. Used to determine the overall accuracy of the placement and classification of the land cover types in each classified image.

$$Accuracy_{Producer,\ Veg.} = \frac{\text{Number of Correct Plots}}{\text{Total Number of Class Plots}} \times 100 \qquad 81.58\% = \frac{31}{38} \times 100$$

Figure 10. Equations for Producer's Accuracy Calculation. Used to determine the producer's accuracy of the placement and classification of the land cover types in each classified image.

$$Accuracy_{User,\ Dev.} = \frac{\text{Number of Correct Plots}}{\text{Total Number of Class Plots}} \times 100 \qquad 100\% = \frac{16}{16} \times 100$$

Figure 11. Equations for User's Accuracy Calculation. Used to determine the user's accuracy of the placement and classification of the land cover types in each classified image.

Classified 2008 Image				
Class 1				
Producer's Accuracy (%)				100
User's Accuracy (%)				95
Class 2				
Producer's Accuracy (%)				96.88
User's Accuracy (%)				100
Overall Classification Accuracy (%)				98.04
Overall Kappa Statistic				0.9585
Conditional Kappa Statistic – Class 1 (Developed)				0.9203
Conditional Kappa Statistic – Class 2 (Vegetation)				1
Error Matrix				
Classed Determined From Reference Image				
	Num. of Points	Developed	Vegetation	**Totals**
Classes Determined From Classified Image	Developed	19	1	20
	Vegetation	0	31	31
	Totals	19	32	**51**
Classified 2016 Image				
Class 1				
Producer's Accuracy (%)				100
User's Accuracy (%)				80
Class 2				
Producer's Accuracy (%)				88.57
User's Accuracy (%)				100
Overall Classification Accuracy (%)				92.16
Overall Kappa Statistic				0.8294
Conditional Kappa Statistic – Class 1 (Developed)				0.7086
Conditional Kappa Statistic – Class 2 (Vegetation)				1
Error Matrix				
Classes Determined From Reference Image				
	Num. of Points	Developed	Vegetation	**Totals**
Classes Determined From Classified Image	Developed	16	4	20
	Vegetation	0	31	31
	Totals	16	35	**51**

Table 9. Statistics by Classified Image. Data acquired upon processing the accuracy assessment for each image. The shaded values in each error matrix represent the points that were classified correctly according to the reference data. The values outside of the diagonal line were misclassified.

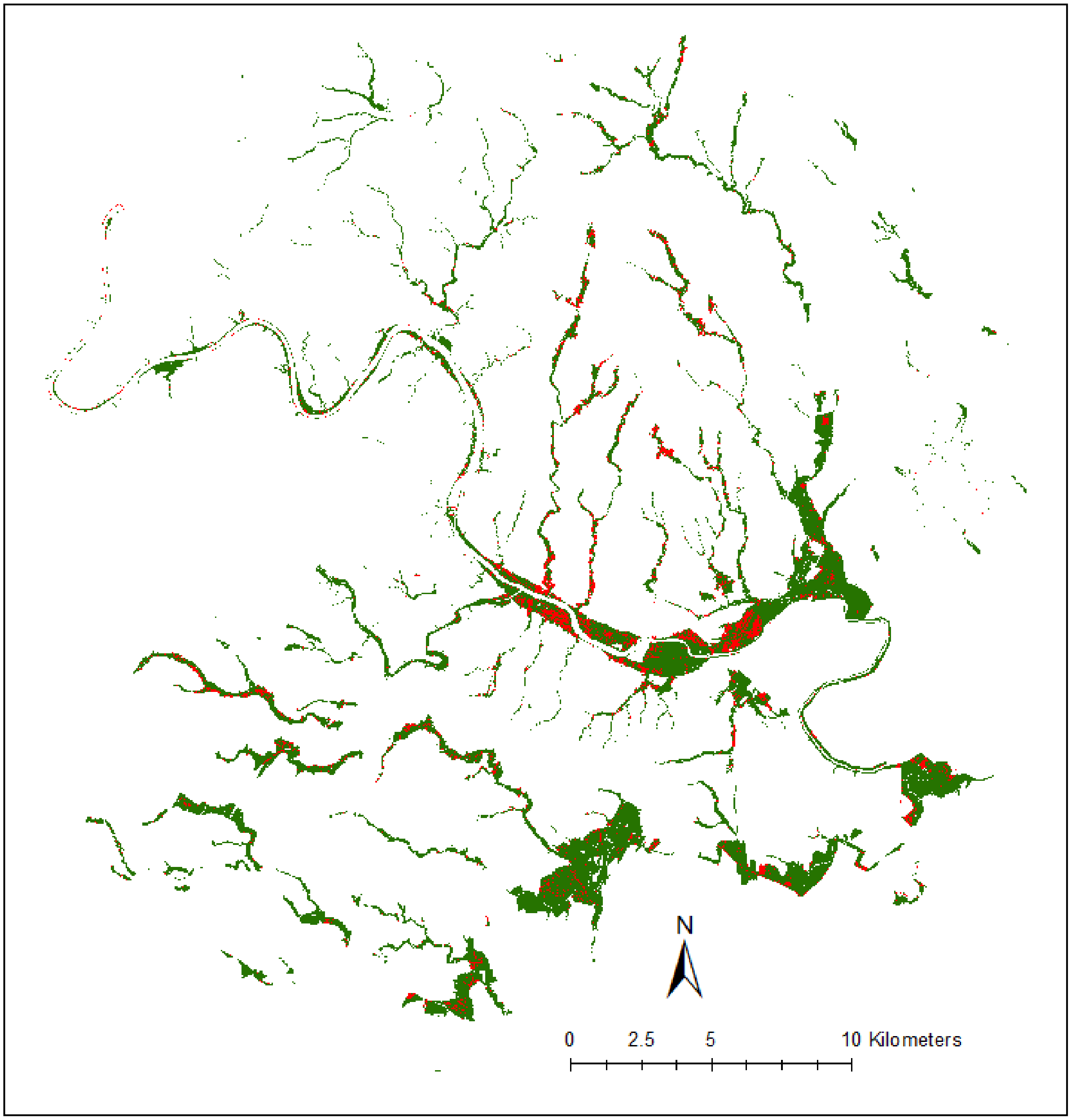

Figure 12. Classification of the Study Area in 2008. The dark green areas represent vegetation and the red areas represent developed land.

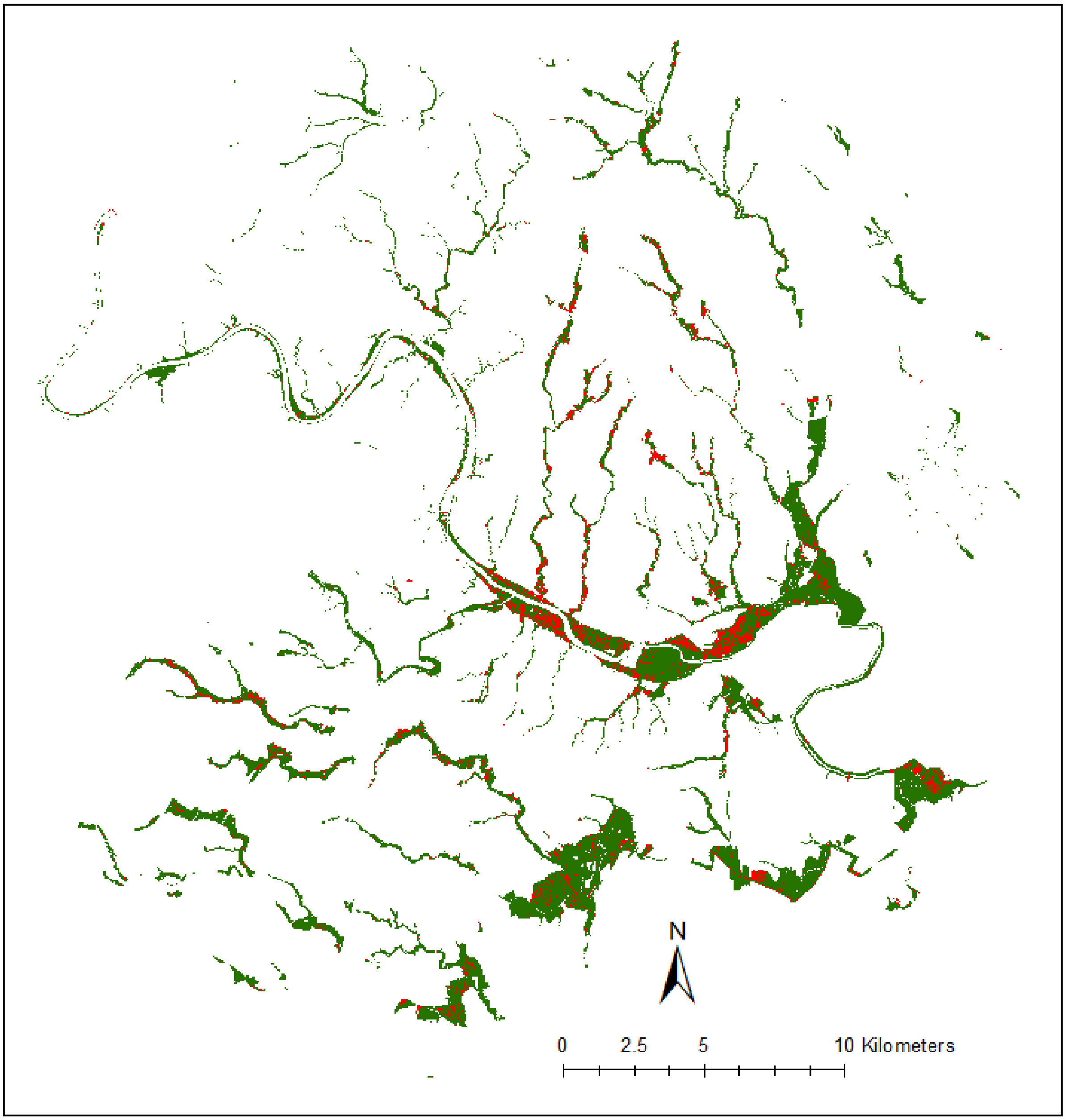

Figure 13. Classification of the Study Area in 2016. The dark green areas represent vegetation and the red areas represent developed land.

Finally, a change detection image and summary file were created by inputting each classified image into the "Matrix Union" function in ERDAS Imagine. The outputs of this step provided visual and statistical information on the thematic changes that occurred across the study area between 2008 and 2016 (Figure 14 and Table 10). As shown in Figure 14, the dark green areas represent vegetation that did not change between 2008 and 2016, and the red areas represent developed land that did not change with the same timeframe. Yellow is used to represent land that changed from developed to vegetation, and turquoise is used to signify land that changed from vegetation to developed. Table 10 displays cross-tabulation statistics useful in comparing the changes, or lack thereof, between the two land cover classes in the each image.

5.3 Limitations

The primary limitation of this study is the difference in multispectral characteristics between the two images used. While the images feature the same spatial resolution, the image from 2008 is CIR with four bands and the image from 2016 is NC with three bands. The differences in multispectral properties have the potential to affect the drawing and placement of AOIs for each type of land cover during the supervised classification process. This limitation explains the slight variance in accuracy between each image (Table 9). In addition, the multispectral signatures of the two forms of land cover likely contributed to the misclassification of smaller water features remaining within the study area upon the extraction of most hydrological elements from the image. Of the remaining smaller water features (i.e. swimming pools, municipal fountains, etc.), their classifications are a result of the land cover that they more closely resemble in either image. The same limitation is true for the misclassification of dry grass for developed land in the image from 2016.

VI. RESULTS

Based on the findings of this study, there is a lack of variety amongst the land cover types throughout the City of Austin's urbanized floodplain. Excluding the water features extracted prior to conducting the classification and analysis, the landscape is comprised of either developed or vegetated land (Figures 2 and 11). In addition, the floodplain has undergone an increase in land cover change and development between the years of 2008 and 2016. As shown in Table 10, 4.71% of vegetated land from 2008 was classified as developed land in 2016. An unexpected finding of this study was the increase in vegetated land that was once previously developed. Almost 30% of developed land from 2008 was classified as vegetated land in 2016. This is likely due to recent floodplain reclamation by public and private entities on or nearby major hydrological features, like the Colorado River.

	Zone Number 1 - Developed		
Class	Change Between Classes	Percentage (%)	Area (km^2)
1	Developed to Developed	71.81	7.20
2	Developed to Vegetation	28.19	2.83
Totals	———	**100**	**10.03**
	Zone Number 2 - Vegetation		
Class	Change Between Classes	Percentage (%)	Area (km^2)
1	Vegetation to Developed	4.71	3.14
2	Vegetation to Vegetation	95.29	63.45
Totals	———	**100**	**66.59**

Table 10. Matrix Union Statistics by Class. Data acquired upon processing the Matrix Union with each classified image. The changes of land cover classes (i.e. pixel counts and land area) between 2008 and 2016 are quantified in this table.

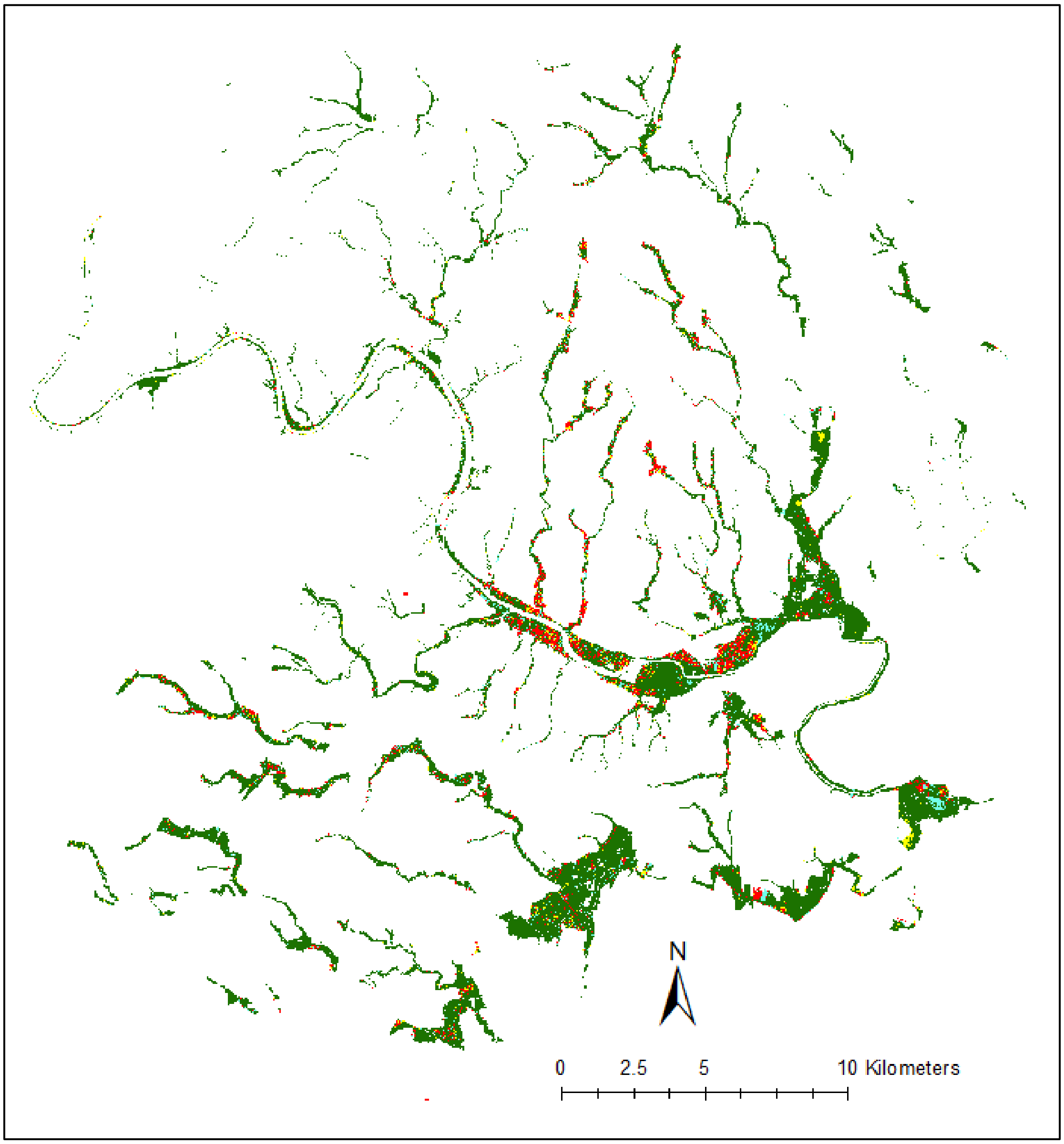

Figure 14. Matrix Union Analysis of Land Cover. The dark green areas represent vegetation that did not change between 2008 and 2016, and the red areas represent developed land that did not change with the same timeframe. Yellow is used to represent land that changed from developed to vegetation, and turquoise is used to signify land that changed from vegetation to developed.

6.1 Geography of the Floodplain

Some portions of the study area did not experience a change in land cover between 2008 and 2016. For example, large sections of Downtown Austin remained developed, which is to be expected within a rapidly urbanizing area (Figure 16). In addition, many roadways, commercial centers, neighborhoods, and housing complexes did not experience a change in land cover throughout the 8-year period. Vegetated land along the downtown periphery and banks of major water features remained unchanged, as well (Figure 15). This is likely due to the lack of concentrated, outward development around the urban core, as well as the increased flood hazards associated with building alongside a lake, river, or stream.

As hypothesized, the 100 and 500-year floodplains experienced a change from vegetated to developed land between 2008 and 2016. The construction of new neighborhoods, housing complexes, roadways, and commercial centers accounted for much of the development within the study area (Figure 17). Portions of land along or near major hydrological bodies, like the Colorado River, changed from developed to vegetated land over the 8-year study period (Figure 18). This alteration is likely due to recent floodplain reclamation efforts by public and private entities in the City of Austin.

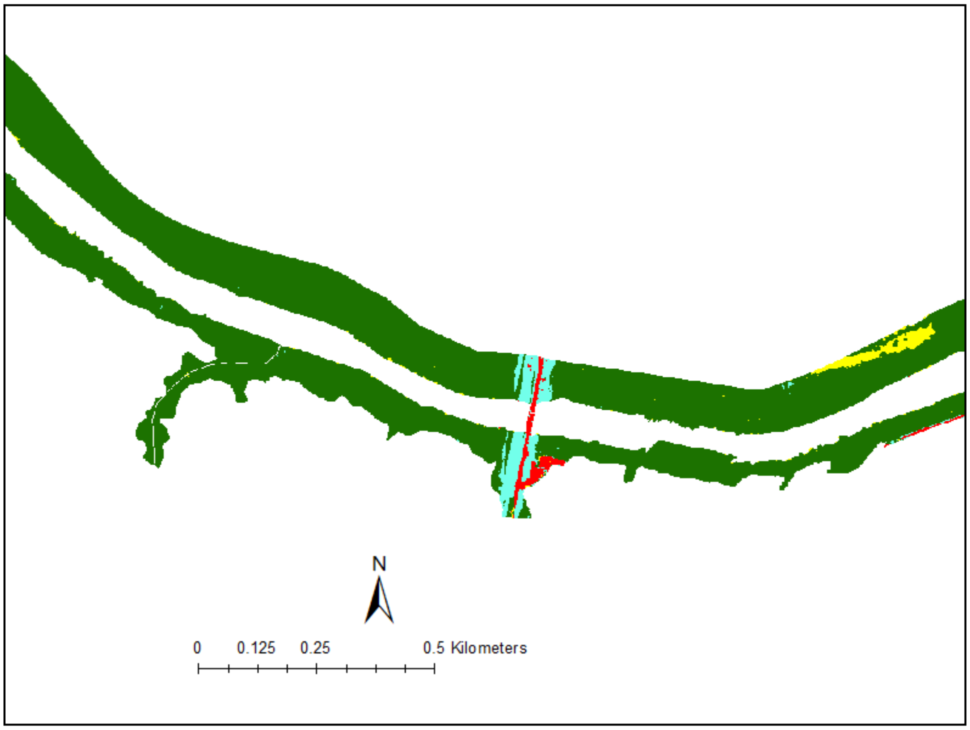

Figure 15. Unchanged Vegetated Land. In this example, the banks and surrounding area of the Colorado River remained vegetated (shown in dark green) between 2008 and 2016.

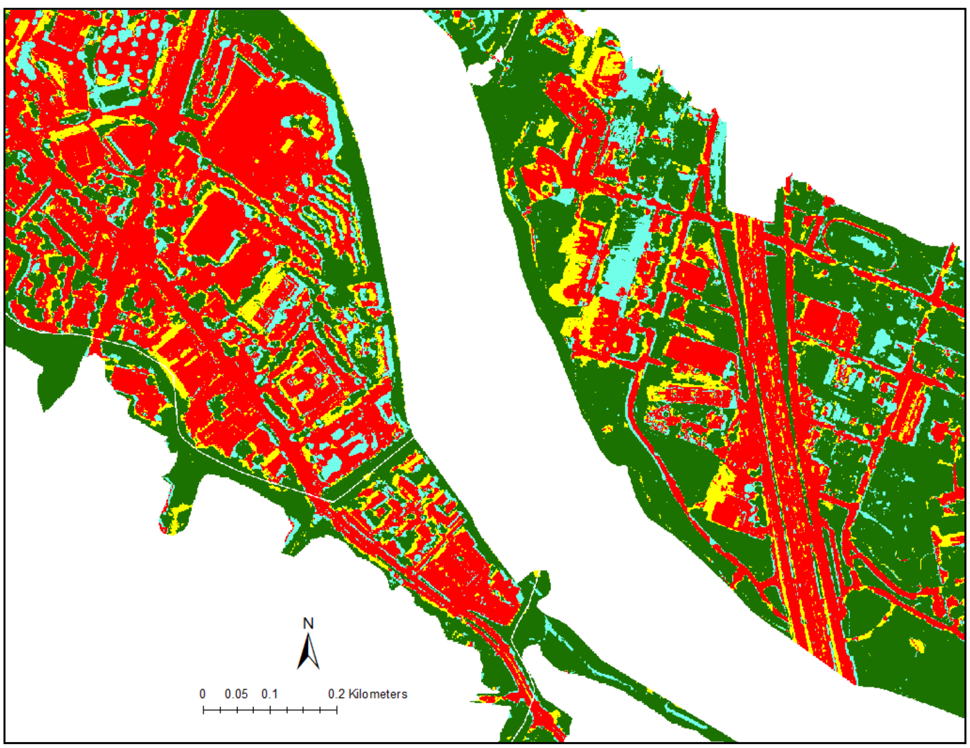

Figure 16. Unchanged Developed Land. In this example, Downtown Austin remained developed (shown in red) between 2008 and 2016.

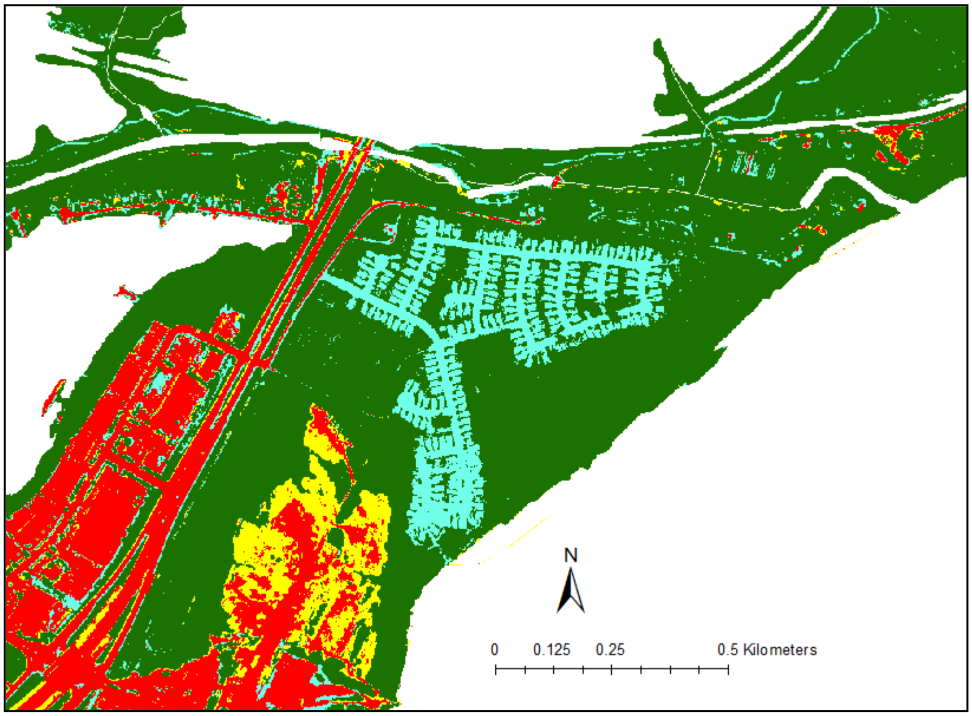

Figure 17. Vegetated Land That Changed to Developed Land. In this example, a new housing development was built (shown in turquoise) near the Colorado River in East Austin.

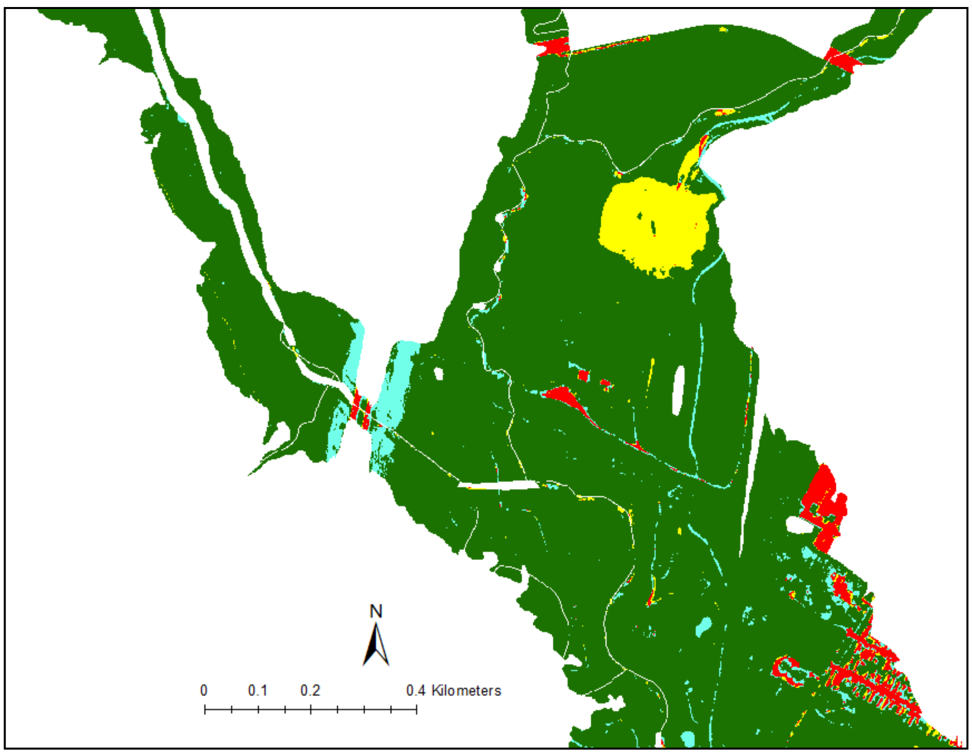

Figure 18. Developed Land That Changed to Vegetated Land. In this example, land was reclaimed (shown in yellow) near the Colorado River between 2008 and 2016.

6.2 Areas for Further Research

The results of this project are applicable to future research involving the City of Austin. Such research may include a flood intensity risk and rate of change assessment for the neighborhoods and communities that exist in more vulnerable or rapidly developing areas within the floodplain. By addressing further research topics, city officials, developers, and residents could gain an even greater understanding of where extreme damage could occur during a major flood event in the urbanized floodplain, as well as who or what may experience both the immediate and longstanding effects.

VII. CONCLUSION

The looming threat of extreme hydrometeorological events on urban areas are an undeniable burden for cities and regions around the world (Kiedrzyńska et al. 2015). As urban environments continue to expand their reach and influence across landscapes, increases in impervious surfaces can exacerbate the potential for extreme flooding (Furl et al. 2015 and Kwak et al. 2008). Because of this, research efforts are needed to explore and analyze the identity and defining characteristics of the more flood-prone portions of developed areas. Although research exists on the effects of various hydrometeorological events in Austin, TX and surrounding areas, a land cover classification and change detection analysis of the city's 100 and 500-year FEMA floodplains have not yet been done.

Through the utilization of remote sensing techniques, geospatial imagery and statistics, and digital mapping, this study examined a small yet significant portion of the topographic elements that exist across the urbanized floodplain and concluded that land cover change has occurred within the study area between 2008 and 2016. Not only has the City of Austin's urbanized floodplain experienced an increase in developed land within the timeframe, some areas (i.e. near or alongside major water features) that were classified as developed land in 2008 changed to vegetated land in 2016. In addition, this study confirmed the lack of variety across forms of land cover within the study area. With the exception of the hydrological features extracted from the images prior to classification and analysis, the study area was comprised of developed and vegetated land.

Given that anthropogenic factors often instigate and intensify flood events, this study provides valuable insight into the presence and distribution of inhabited and uninhabited land across a flood-prone landscape (Glosińska 2014 and Green et al. 2000). With growing concerns surrounding the impending threats of climate change on heavily populated and expanding urban environments, I believe that officials, developers, residents in the City of Austin could greatly benefit from the results of this study. Equipped with an improved understanding of what actually exists in the floodplain, I hope that they will then be prepared to make sensible decisions concerning future efforts in land development and flood hazard mitigation and management.

VIII. REFERENCES

Anderson, J. R., Hardy, E. E., Roach, J. T., and Witmer, R.E. 1976. A Land Use And Land Cover Classification System For Use With Remote Sensor Data. *U.S. Geological Survey Circular 671*.

Antonie, J., Fischer, G., and Makowski, M. 1997. Multiple criteria land use analysis. *Applied Mathematics and Computation* 85:195-215.

Aubrecht, C., Kostl, M., Knoflacher, M., Steinnocher, K. 2010. The importance of active public communication – Settlement systems and land use patterns seen from a disaster perspective. CORP 2009 Proceedings, 14th International Conference on Urban Planning, Regional Development, and Information Society-Strategies.

City-Data.com, http://www.city-data.com/us-cities/The-South/Austin-Geography-and-Climate.html (Accessed 10 February 2017).

City of Austin. 2017. Annexation. *Austin Planning and Zoning Department*. The Official Website for the City of Austin. http://www.austintexas.gov/department/annexation. (Accessed 20 April 2017).

______ . 2017a. *Austin Watershed Protection Department*. The Official Website for the City of Austin. https://www.austintexas.gov/faq/1-what-floodplain. (Accessed 12 December 2016).

______ . 2017b. Top 10 Demographic Trends. *Austin Planning and Zoning Department*. The Official Website for the City of Austin. http://www.austintexas.gov/page/top-ten-demographic-trends-austin-texas. (Accessed 10 February 2017).

______ . 2017c. The Music Office. *Austin Convention and Visitor's Bureau*. http://www.austintexas.org/. (Accessed 10 February 2017).

Congalton, R.G. 1991. A Review of Assessing the Accuracy of Classifications of Remotely Sensed Data. *Remote Sensing of Environment* 37 (1):35-46.

Cornell Law Review. 2014. *What is Extraterritorial Jurisdiction?* http://cornelllawreview.org/articles/what-is-extraterritorial-jurisdiction/. (Accessed 20 April 2017).

Floodsite Project. 2017. *What is Flood Risk?* http://www.floodsite.net/juniorfloodsite/html/en/student/thingstoknow/geography/risk1.html. (Accessed 20 April 2017).

Flood Risk Management. 2017. *What is Flood Risk?* http://www.ioutsidedesign.co.uk/Case%20studies/FCRM/section5_1.html. (Accessed 20 April 2017).

Foody, G.M. 2002. Status of Land Cover Classification Accuracy Assessment. *Remote Sensing of Environment* 80(1):185-201.

Forbes. 2016. *America's Next Great Metropolis is Taking Shape in Texas*. https://www.forbes.com/sites/joelkotkin/2016/10/13/the-next-great-american-metropolis-is-taking-shape-in-texas/#45d76f731e2f. (Accessed 10 February 2017).

______. 2016a. *America's Fastest Growing Cities 2016*. https://www.forbes.com/pictures/emeg45ehgji/1-austin-texas/#bdf9f402726d. (Accessed 10 February 2017).

Furl, C., H. O. Sharif, A. E. Hassan, N. Mazari, D. Burtch, and G. L. Mullendore. 2015. Hydrometeorological Analysis of Tropical Storm Hermine and Central Texas Flash Flooding. *Journal of Hydrometeorology* 16(6):2311–2327.

Glosińska, E. 2014. Floodplain Management in the Context of Assessment and Changes of Flood Risk and the Environment – a Review. *Polish Journal on Environmental Studies* 23(6):1895–1904.

Gonçalves R.P., Assis L.C., Vieira, C.A.O. 2007. Comparison of Sampling Methods to

Classification of Remotely Sensed Images. Simpósio Internacional de Agricultura de Precisão.

Green, C. H., Parker, D. J., and Tunstall, S. M. 2000. Assessment of Flood Control and Management Options. Thematic Review IV.4 prepared as an input to the World Commission on Dams, Cape Town, www.dams.org.

Humboldt State University. Supervised Classification. http://gsp.humboldt.edu/olm_2015/Courses/GSP_216_Online/lesson6-1/supervised.html. (Accessed 16 April 2018).

Kiedrzyńska, E., M. Kiedrzyński, and M. Zalewski. 2014. Sustainable floodplain management for flood prevention and water quality improvement. *Natural Hazards* 76(2):955–977.

Kourgialas, N. N.and Karatzas, G. P. 2011. Flood management and a GIS modelling method to assess flood-hazard areas – a case study. *Hydrol. Sci.* 56(2), 212-225.

Kwak, Y. and Kondoh, A. 2008. A study on the extraction of multi-factor influencing floods from RS image and GIS data; a case study in Nackdong basin, S. Korea. *The International Archives of the Photogrammetry, Remote Sensing and Spatial Information Sciences* XXXVII(PartB8), 421-426.

Li, C., X. Cheng, N. Li, X. Du, Q. Yu, and G. Kan. 2016. A Framework for Flood Risk Analysis and Benefit Assessment of Flood Control Measures in Urban Areas. *International Journal of Environmental Research and Public Health* 13.

Ndabula, C., G. G. Jidauna, K. Oyatayo, P. D. Averik, and E. O. Iguisi. 2012. Analysis of

Urban Floodplain Encroachment: Strategic Approach to Flood and Floodplain Management in Kaduna Metropolis, Nigeria. *Journal of Geography and Geology* 4(1).

Nel, J. L., D. C. Le Maitre, D. C. Nel, B. Reyers, S. Archibald, B. W. van Wilgen, G. G. Forsyth, A. K. Theron, P. J. O'Farrell, J. Kahinda, F. A. Engelbrecht, E. Kapangaziwiri, L. van Niekerk, and L. Barwell. 2014. Natural Hazards in a Changing World: A Case for Ecosystem-Based Management. *PLOS ONE* 9.

Singh, A. 1989. Digital Change Detection Techniques Using Remotely-Sensed Data. *International Journal of Remote Sensing* 10(6):989-1003.

Sisodia, P.S., Tiwari, V., Kumar, A. 2014. Analysis of Supervised Maximum Likelihood Classification for Remote Sensing Image. IEEE International Conference on Recent Advances and Innovations in Engineering.

Texas Natural Resource Information System. *StratMap Orthoimagery*. https://tnris.org/stratmap/orthoimagery/. (Accessed 21 March 2018).

Texas State Historical Association. *Physical Regions of Texas*. http://texasalmanac.com/ topics/environment/physical-regions-texas. (Accessed 10 February 2017).

U.S. News and World Report. 2017. *U.S. News and World Report Unveils the 2017 Best Places to Live*. https://www.usnews.com/info/blogs/press-room/articles/2017-02-07/us-news-unveils-the-2017-best-places-to-live. (Accessed 10 February 2017).

United States Census Bureau. https://www.census.gov/quickfacts/table/PST045215/ 4805000. (Accessed 10 February 2017).

United States Department of Agriculture. *NAIP Imagery*. https://www.fsa.usda.gov/ programs-and-services/aerial-photography/imagery-programs/naip-imagery/.

(Accessed 23 March 2018).